Dye-sensitized Solar Cell Fabricated by Electrostatic Layer-by-Layer Assembly of Amphoteric TiO2 Nanoparticles

ARTICLE *in* LANGMUIR · FEBRUARY 2003

Impact Factor: 4.46 · DOI: 10.1021/la020639b

5 AUTHORS, INCLUDING:

Jayant Kumar
University of Massachusetts Lowell
516 PUBLICATIONS **10,809** CITATIONS

Dye-sensitized Solar Cell Fabricated by Electrostatic Layer-by-Layer Assembly of Amphoteric TiO_2 Nanoparticles

Jin-An He,[†] Ravi Mosurkal,[†] Lynne A. Samuelson,*[,‡] Lian Li,[†] and Jayant Kumar*[,†]

Center for Advanced Materials, University of Massachusetts Lowell, Lowell, Massachusetts 01854, and Natick Soldier Center, U.S. Army Soldier & Biological Chemical Command, Natick, Massachusetts 01760

Received July 15, 2002. In Final Form: December 2, 2002

Nanocrystalline TiO_2 amphoteric colloidal charged particles and polyelectrolytes have been used to fabricate a dye-sensitized solar cell. Two weak polyelectrolytes, poly(allylamine hydrochloride) and poly(acrylic acid), and two strong polyelectrolytes, poly(dimethyldiallylammonium chloride) (PDAC) and poly(sodium 4-styrenesulfonate), have been utilized to assemble polyion/TiO_2 nanocomposite multilayered films by the electrostatic layer-by-layer deposition technique. The layer-by-layer assembly of the TiO_2 nanoparticles proceeds linearly as shown by sequential UV−vis absorption and thickness measurements. The morphology of these assemblies was characterized using atomic force microscopy. The nanoporous polyion/TiO_2 films were sintered and used as working electrodes for *cis*-di(thiocyanato)-*N*,*N*-bis(2,2′-bipyridyldicarboxylate)-ruthenium(II) (N3) sensitized solar cells. *I*−*V* characteristics of the solar cells made by the calcinated polyelectrolyte/TiO_2 electrodes show several interesting results. (i) The short-circuit current does not linearly increase with the thickness of the TiO_2 electrode, even though the adsorption behavior of the N3 dye shows a linear increase. (ii) The precursor polyelectrolytes used to assemble TiO_2 play a major role in the photovoltaic performance of the solar cells. Thermogravimetric analysis studies show that the thermal stability of the polyelectrolytes may have a direct effect on the overall device efficiency. (iii) The photovoltaic performance of these solar cells is comparable to that of cells made by other methods such as spin casting, the layer-by-layer technique offers unsurpassed control in manipulating the final device thickness. An efficiency of 7.2% was obtained for the solar cell made from PDAC/TiO_2 (200 bilayers) precursor film, under 1 sun at simulated Air Mass 1.5 direct irradiation.

1. Introduction

Since the report of highly efficient (∼10%) dye-sensitized solar cells (DSSCs) by Grätzel, DSSCs have become the most promising alternative to conventional silicon solar cells and are currently under extensive investigation.[1] One of the key components of DSSCs is the nanocrystalline semiconductor electrode, which can normally be fabricated by several wet chemical methods such as casting, doctor blading, and screen printing as well as different physical methods including sputtering and chemical vapor deposition.[2] The challenge to precisely control the composition, porosity, and film thickness at the nanoscale still remains. To address this, we have modified the electrostatic layer-by-layer (ELBL) deposition technique[3] to prepare the TiO_2 semiconductor electrode and optimize the potential of the nanocomposite films for light harvesting and charge transfer in solar cells.

The ELBL deposition technique using polyelectrolyte templates has evolved as a general approach for film fabrication of charged materials. Recently, this technique has been realized in optoelectronics for the fabrication of organic light-emitting diodes (LEDs),[4] diode junctions,[5] and rectifying junctions.[6] The principle of the ELBL assembly is relatively simple, and it has emerged as a technique for developing well-defined multilayers of mesoscopic structures. When a substrate is alternatively dipped into a pair of aqueous solutions with oppositely charged materials, the materials are electrostatically attracted to each other and sequentially adsorbed on the substrate to form supramolecular assemblies. The ELBL technique provides molecular-level control over the thickness, structure, and composition of multilayer films with rather simple benchmark operation.

Several research groups have employed the ELBL method to assemble wide-band-gap semiconductor nanoparticles such as TiO_2 and ZrO_2 for potential applications in optical, electronic, and mechanical devices.[7] Very recently, this assembly technique has been extended to photovoltaics. Fullerene-linked polyelectrolytes have been

[†] University of Massachusetts Lowell.

[‡] Natick Soldier Center.

(1) (a) Nazeeruddin, M. K.; Kay, A.; Rodicio, I.; Humphry-Baker, R.; Muller, E.; Liska, P.; Vlachopoulos, N.; Grätzel, M. *J. Am. Chem. Soc.* **1993**, *115*, 6382. (b) Nazeeruddin, M. K.; Pechy, P.; Renouard, T.; Zakeeruddin, S. M.; Humphry-Baker, R.; Comte, P.; Liska, P.; Cevey, L.; Costa, E.; Shklover, V.; Spiccia, L.; Deacon, G. B.; Bignozzi, C. A.; Grätzel, M. *J. Am. Chem. Soc.* **2001**, *123*, 1613. (c) Grätzel, M. *Nature* **2001**, *414*, 338.

(2) (a) Suzuki, S. *Thin Solid Films* **1999**, *351*, 194. (b) Lee, W. G.; Woo, S. I.; Kim, J. C.; Choi, S. H.; Oh, K. H. *Thin Solid Films* **1994**, *237*, 105. (c) O'Regan, B.; Grätzel, M. *Nature* **1991**, *353*, 737.

(3) Decher, G. *Science* **1997**, *277*, 1232.

(4) (a) Wu, A.; Yoo, D.; Lee, J.-K.; Rubner, M. F. *J. Am. Chem. Soc.* **1999**, *121*, 4883. (b) Ho, P.; Kim, J.-S.; Burroughes, J. H.; Becker, H.; Li, S. F. Y.; Brown, T. M.; Cacialli, F.; Friend, R. H. *Nature* **2000**, *404*, 481.

(5) (a) Cassagneau, T.; Mallouk, T. E.; Fendler, J. H. *J. Am. Chem. Soc.* **1998**, *120*, 7848. (b) Cassagneau, T.; Fendler, J. H.; Johnson, S. A.; Mallouk, T. E. *Adv. Mater.* **2000**, *12*, 1363.

(6) Kovtyukhova, N. I.; Martin, B. R.; Mbindyo, J. K. N.; Smith, P. A.; Razavi, B.; Mayer, T. S.; Mallouk, T. E. *J. Phys. Chem. B* **2001**, *105*, 8762.

(7) (a) Rosidian, A.; Liu, Y. J.; Claus, R. *Adv. Mater.* **1998**, *10*, 1087. (b) Kovtyukhova, N.; Ollivier, P. J.; Chizhik, S.; Dubravin, A.; Buzaneva, E.; Gorchinskiy, A.; Marchenko, A.; Smirnova, N. *Thin Solid Films* **1999**, *337*, 166. (c) Sasaki, T.; Ebina, Y.; Tanaka, T.; Harada, M.; Watanabe, M. *Chem. Mater.* **2001**, *13*, 4661.

10.1021/la020639b CCC: $25.00
Published on Web 02/07/2003

Chart 1. Chemical Structures of the Polyelectrolytes and Dye Used

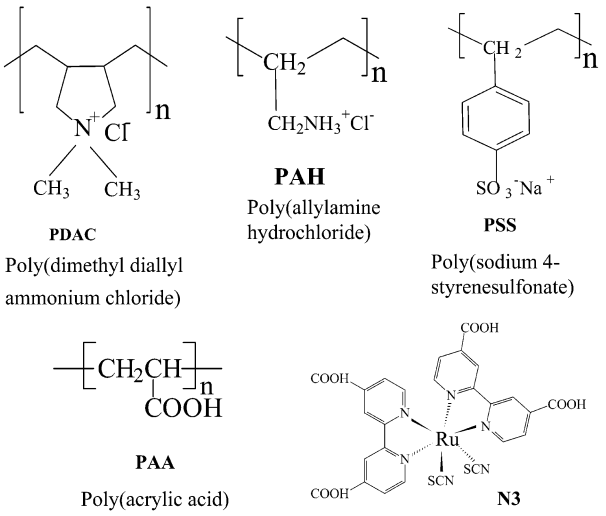

synthesized and layered with other polyelectrolytes such as a poly(*p*-phenylene vinylene) precursor to form layer-by-layer films of donor−acceptor structures.[8] However, these solid-state solar cells, with evaporated thin metal layers as electrodes, generally show very poor overall photoelectric conversion efficiency. In this work, the ELBL method was used to make TiO_2/polyion composite films. After sintering, the TiO_2 film was sensitized by *cis*-di(thiocyanato)-*N*,*N*-bis(2,2′-bipyridyldicarboxylate)-ruthenium(II) (N3) and solar cells were fabricated. The effects of different polyions, the thickness of the ELBL assemblies, on the final conversion efficiency of the solar cells are discussed.

2. Experimental Section

2.1. Materials and Method. Poly(acrylic acid) (PAA; average M_W, ca. 450K), poly(diallyldimethylammonium chloride) (PDAC; average M_W, ca. 200−350K), poly(sodium 4-styrenesulfonate) (PSS; average M_W, ca. 70K), and poly(allylamine hydrochloride) (PAH; average M_W, ca. 50−65K) were purchased from Aldrich Chemical Co. and used as received. Anatase nanocrystalline TiO_2 particles (average particle size, 32 nm) was obtained from Alfa Aesar. ′N3 was synthesized according to the reported procedure.[1] The chemical structures of the compounds used in our work are shown in Chart 1. Milli-Q water with a resistivity of >15 MΩ cm was used as the solvent throughout the self-assembly experiments.

Absorption spectra were measured on a Perkin-Elmer Lambda-9 UV/vis/near-infrared spectrophotometer. Atomic force microscope (AFM) images were obtained using an AFM (Park Scientific, CA) operated in the noncontact mode using a standard silicon nitride cantilever (force constant, 0.03 N/m) in ambient air. The scan frequency was 1 Hz. The thickness of the films was measured with a Solan dektek IIA profilometer. Quartz slides were used for absorption, fluorine-doped SnO_2 glass slides were used for photovoltaic and thickness measurements, and silicon wafers were used for atomic force microscopy. Thermogravimetric analysis (TGA; Hi-Res TGA 2950 analyzer, TA Instruments) was carried out in ambient atmosphere, which mimics the sintering condition. TGA curves were recorded by heating solid samples (∼5 mg) at a rate of 10 °C/min up to 700 °C.

2.2. Preparation of Polyelectrolyte/TiO_2 Film. TiO_2 nanoparticles are amphoteric in nature, and the charge can be controlled by adjusting the pH of the colloidal suspension below or above the isoelectric point of TiO_2. Nanocomposite polycation/TiO_2 multilayer films were prepared via the ELBL technique by using either a pH 6.4 PDAC or a pH 9.0 PAH solution as positively charged binders with TiO_2 as negatively charged particles and dispersing it into a pH 10, 10 mM Na_2CO_3−$NaHCO_3$ buffer solution. Composite polyanion/TiO_2 films were fabricated by using pH 5.0 PAA or pH 4.0 PSS as negatively charged binders with TiO_2 as positively charged particles in suspension in pH 2.5 (adjusted by 1 M HCl) aqueous solution. In all cases, pH was adjusted by 1 M NaOH and 1 M HCl except where specifically mentioned. The sequential adsorption in 0.2 wt % TiO_2 and 1 mg/mL polyelectrolyte aqueous solutions to form polyelectrolyte/TiO_2 multilayers was carried out using an HMS series programmable slide stainer apparatus (Carl Zeiss, Inc.). F-Doped SnO_2 conducting glass was first immersed into the solution containing positively charged species for 5 min. After rinsing twice in water (2 min in each bath with agitation) and drying in air for 5 min, the modified substrate was then transferred into the solution containing the negatively charged species for 5 min, agitated, washed twice with water, and then dried for 5 min. The above procedures were repeated until a film of the desired thickness was obtained. In the adsorption process, the 0.2 wt % TiO_2 colloidal suspension was constantly stirred to ensure a homogeneous dispersion without precipitate. The diagram to explain the fabrication procedure is shown in Chart 2.

2.3. Preparation of DSSCs and Photovoltaic Measurements. The ELBL-assembled polyelectrolyte/TiO_2 composite films were heated in air for 30 min at 550 °C to obtain sintered TiO_2 nanoporous films. To minimize rehydration of TiO_2 from moisture in the ambient air, the electrodes were immersed into a 0.5 mM N3 ethanol solution overnight while still warm (100−120 °C) from the annealing step. After dye adsorption, the electrodes were washed by ethanol and air-dried. A sandwiched photovoltaic device was prepared with the N3-sensitized TiO_2 electrode and a platinum (Pt) counter electrode. Pt counter electrodes with a mirror finish were prepared by electron beam deposition of a 60 nm layer of Pt on top of a 30 nm layer of Ti on a SnO_2 conducting glass. The active area of all cells was approximately 0.25 cm^2. The thickness of the TiO_2 layer was precisely controlled, from 1 to 8 μm, depending on the number of dipping cycles used. The electrolyte, which was introduced into the interior of the photovoltaic cell via capillary forces, consisted of 1.0 M LiI, 0.1 M iodine, and 2.0 M 4-*tert*-butylpyridine in acetonitrile.

The current−voltage ($I-V$) characteristics of the solar cell were carried out using a Keithley 2400 SourceMeter, which was controlled by a program written in TestPoint. An Oriel 1000 W xenon lamp served as the light source in combination with one ultraviolet long pass filter (cut-on wavelength, 324 nm), one water filter, and one heat-absorbing filter to remove ultraviolet and infrared radiation. The Oriel Air Mass (AM) 0 filter and AM 1.5 direct filter were placed in the optical path to simulate AM 1.5 Direct solar irradiance. The light intensity was measured by an Oriel radiant power energy meter with a thermopile detector. All experiments were performed at AM 1.5 Direct irradiation at 100 mW/cm^2 light intensity. The cell performance parameters, including short-circuit current (Isc), open-circuit voltage (Voc), maximum output power (Pmax), fill factor (FF = Pmax/(IscVoc)), and cell efficiency (η = IscVocFF/total incident energy × 100%), were measured and calculated from the $I-V$ characteristics.

The amount of adsorbed dye on the different polyelectrolyte/TiO_2 films was determined by desorbing N3 from the sensitized film into a solution of 20 mM Na_2CO_3−$NaHCO_3$ buffer (pH 9.9) and measuring its absorption spectrum. The absorption peaks of N3 in 20 mM Na_2CO_3−$NaHCO_3$ buffer are located at 369 and 498 nm. The molar absorption coefficient of N3 at 498 nm in the buffer was determined to be 1.35×10^4 M^{-1} cm^{-1}.

3. Results and Discussion

3.1. Fabrication and Characterization of Polyelectrolyte/TiO_2 Films. The nature of the surface charge

(8) (a) Piok, T.; Brands, C.; Neyman, P. J.; Erlacher, A.; Soman, C.; Murray, M. A.; Schroeder, R.; Graupner, W.; Heflin, J. R.; Marciu, D.; Drake, A.; Miller, M. B.; Wang, H.; Gibson, H.; Dorn, H. C.; Leising, G.; Guzy, M.; Davis, R. M. *Synth. Met.* **2001**, *116*, 343. (b) Baur, J. W.; Durstock, M. F.; Taylor, B. E.; Spry, R. J.; Reulbach, S.; Chiang, L. Y. *Synth. Met.* **2001**, *121*, 1547. (c) Luo, C. P.; Guldi, D. M.; Maggini, M.; Menna, E.; Mondini, S.; Kotov, N. A.; Prato, M. *Angew. Chem., Int. Ed.* **2000**, *39*, 3905. (d) Durstock, M. F.; Taylor, B.; Spry, R. J.; Chiang, L.; Reulbach, S.; Heitfeld, K.; Baur, J. W. *Synth. Met.* **2001**, *116*, 373. (e) Mattoussi, H.; Rubner, M. F.; Zhou, F.; Kumar, J.; Tripathy, S. K.; Chiang, L. Y. *Appl. Phys. Lett.* **2000**, *77*, 1540.

Chart 2. Formation of Polyion/TiO_2 Nanocomposite Films by the ELBL Method and DSSC Electrode Fabrication

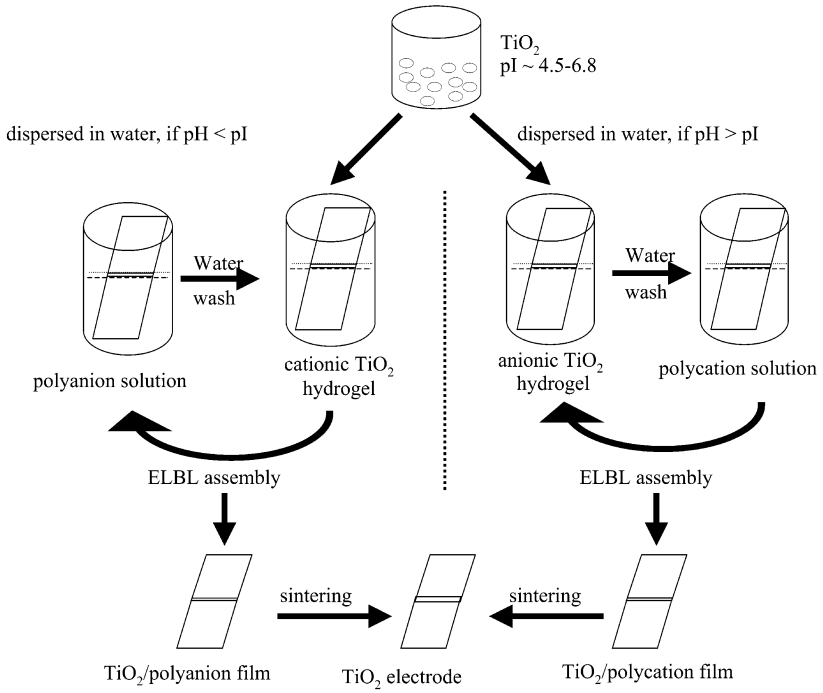

on colloidal TiO_2 nanoparticles is crucial for the assembly of the polyelectrolyte/TiO_2 composite films when the ELBL technique is used. For example, organic acid capped TiO_2 particles are negatively charged ions due to the outermost carboxylic acid group of the stabilizer. These negatively charged particles may then form composite films with polycationic PDAC or PAH by the ELBL method.[5b,9] Another example includes TiO_2 particles prepared under an acidic medium that are positively charged and can adsorb to negatively charged PSS to form PSS/TiO_2 multilayered films.[10] In principle, since the isoelectric point (pI) of an aqueous colloidal TiO_2 dispersion varies from 4.5 to 6.8, depending on the particle size and counterions used,[11] bare TiO_2 nanoparticles may serve as an amphoteric material depending on the pH of the dispersing agent. If the pH of the medium is higher than the pI of the TiO_2, the surface charge of TiO_2 particles is negative. On the other hand, if the medium pH is less than the pI of TiO_2, the particles are positively charged. In this work, by simply adjusting the medium pH, the TiO_2 nanoparticles can be specifically charged to electrostatically layer with either polycations such as PDAC and PAH or polyanions such as PSS and PAA. By use of this approach, both polycation/TiO_2 and polyanion/TiO_2 composite films were prepared by the ELBL method.

Parts a and b of Figure 1 give the UV−vis absorption spectra for the multilayers prepared by sequential deposition of PDAC/TiO_2 bilayers and PSS/TiO_2 bilayers, respectively. As shown, the multilayer adsorption processes are linear and reproducible for sequential deposition cycles for both systems. The absorbance at 300 nm for the PDAC and 270 nm for the PSS is observed to increase linearly with the number of bilayers, as shown in the insets of Figure 1. These results confirm the regular stepwise growth of the films. When the polyelectrolytes PAH or PAA were substituted, a similar linear adsorption behavior was also observed (data not shown). With the continuous growth of the polyion/TiO_2 films, the absorptions of these films become dominated by the light scattering effect from the nanosized TiO_2 particles. As an example, Figure 2 shows the absorption spectra of thicker PDAC/TiO_2 films.

By use of the ELBL assembly procedure, highly reproducible polyelectrolyte/TiO_2 nanocomposite films with controlled thickness were obtained. The measurement of film thickness with the number of bilayers was carried out, and the results are shown in Figure 3. As shown for all polyelectrolytes used, the film thickness increases linearly with the stepwise growth of the polyelectrolyte/TiO_2 bilayers. The bilayer thicknesses are generally larger for the polycations as binders (37 nm per PDAC/TiO_2 and 48 nm per PAH/TiO_2 bilayer) than for the polyanions (18 nm per PSS/TiO_2 and 19 nm per PAA/TiO_2 bilayer). The interesting point here is that the weak polyelectrolytes PAH and PAA give relatively thicker films compared to the strong polyelectrolytes PDAC and PSS. This can be explained according to Shiratori's work about the pH-dependent thickness when using weak polyelectrolytes in the ELBL assembly.[12] At the pHs used in our experiments for PAH (pH 9) and PAA (pH 5), the charge densities of the polyelectrolytes are low, forming thick polyelectrolyte layers. This generally facilitates adsorbing more TiO_2 particles in the sequential assembly. On the other hand, since the average TiO_2 particle size is 32 nm, the TiO_2 coverage in the bilayer for the polycation/TiO_2 films is more than 100% due to possibility of TiO_2 aggregation, and the TiO_2 coverage for the polyanion/TiO_2 film is approximately 60%. This thickness and coverage difference may be explained by the different charge densities of TiO_2 nanoparticles and polyelectrolytes in various pH mediums since the same concentrations and adsorption time were used for each of the polyelectrolytes.

Figure 4 shows AFM images of one bilayer of the PSS/TiO_2 film (Figure 4a) and one bilayer of the PDAC/TiO_2 film (Figure 4b) before sintering. In the polycation system,

(9) Cassagneau, T.; Fendler, J. H.; Mallouk, T. E. *Langmuir* **2000**, *16*, 241.

(10) Liu, Y. J.; Wang, A. B.; Claus, R. *J. Phys. Chem. B* **1997**, *101*, 1385.

(11) (a) Kormann, C.; Bahnemann, D. W.; Hoffmann, M. R. *J. Phys. Chem.* **1988**, *92*, 5196. (b) Zhao, J. C.; Hidaka, H.; Takamura, A.; Pelizzetti, E.; Serpone, N. *Langmuir* **1993**, *9*, 1646.

(12) Shiratori, S. S.; Rubner, M. F. *Macromolecules* **2000**, *33*, 4213.

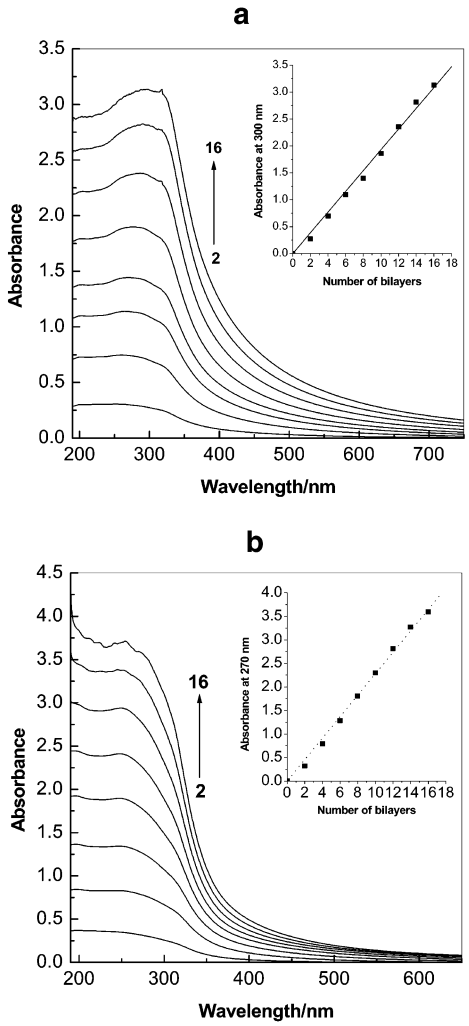

Figure 1. UV−vis absorption spectra of PDAC/TiO_2 (a) and PSS/TiO_2 (b) multilayers on quartz slides. The curves, from bottom to top, correspond to adsorption of 2, 4, 6, 8, 10, 12, 14, and 16 bilayers. The insets show the increases of absorbances at 300 and 270 nm with the number of bilayers.

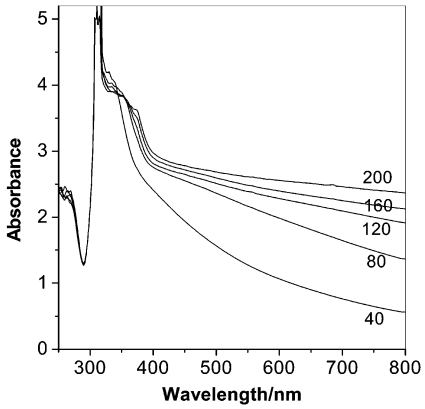

Figure 2. UV−vis absorption spectra of PDAC/TiO_2 multilayered films on F-doped SnO_2 conducting glass. The curves, from bottom to top, correspond to adsorption of 40, 80, 120, 160, and 200 bilayers. The strong light scattering effect comes from the buildup of TiO_2 nanoparticles in the films.

the TiO_2 particles are seen to be more compact with some stacking, while for the polyanion system, the TiO_2 particles aggregate to form islands on the polyelectrolyte film and leave some gaps. The AFM morphological observations here are in accordance with the thickness measurements.

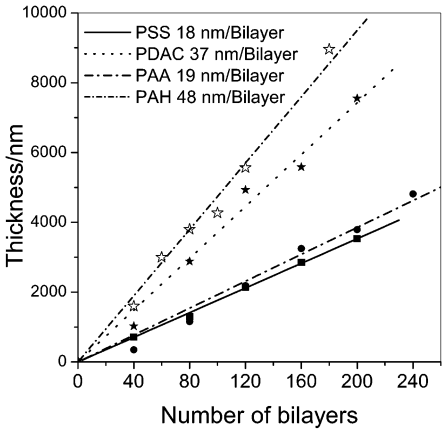

Figure 3. Linear increase of multilayer thickness with the number of deposition cycles of alternating polyion/TiO_2 adsorption.

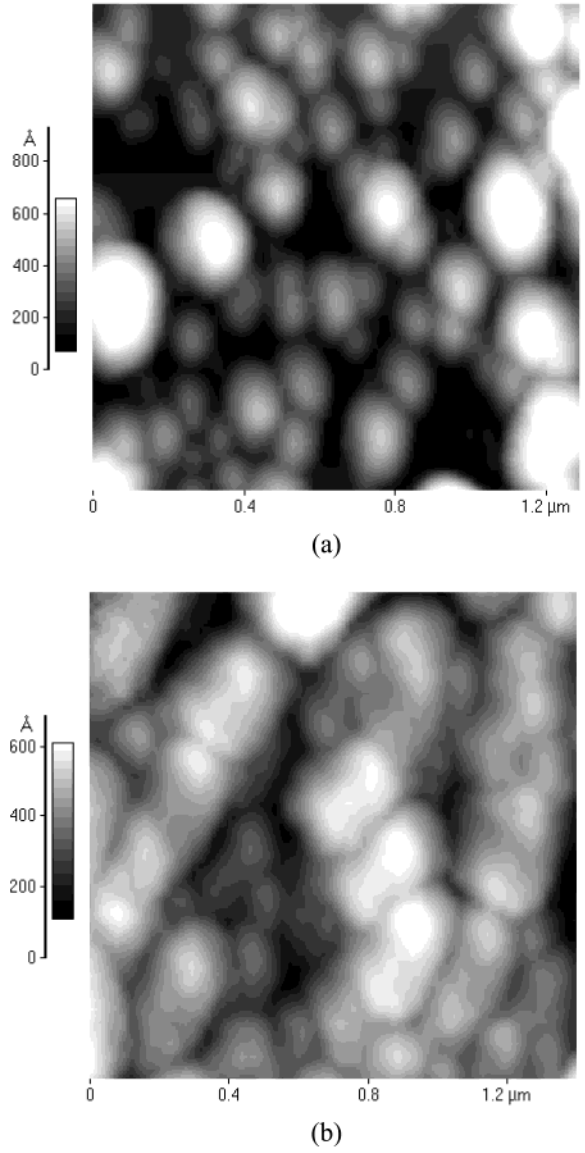

Figure 4. AFM images of (a) one bilayer of PSS/TiO_2 and (b) one bilayer of PDAC/TiO_2 nanocomposite film.

Since the morphology of the polyelectrolyte/TiO_2 films after sintering may directly affect the cell efficiency, we investigated the AFM images of the multilayered films. The results for 120 bilayers of (PSS/TiO_2) film before and

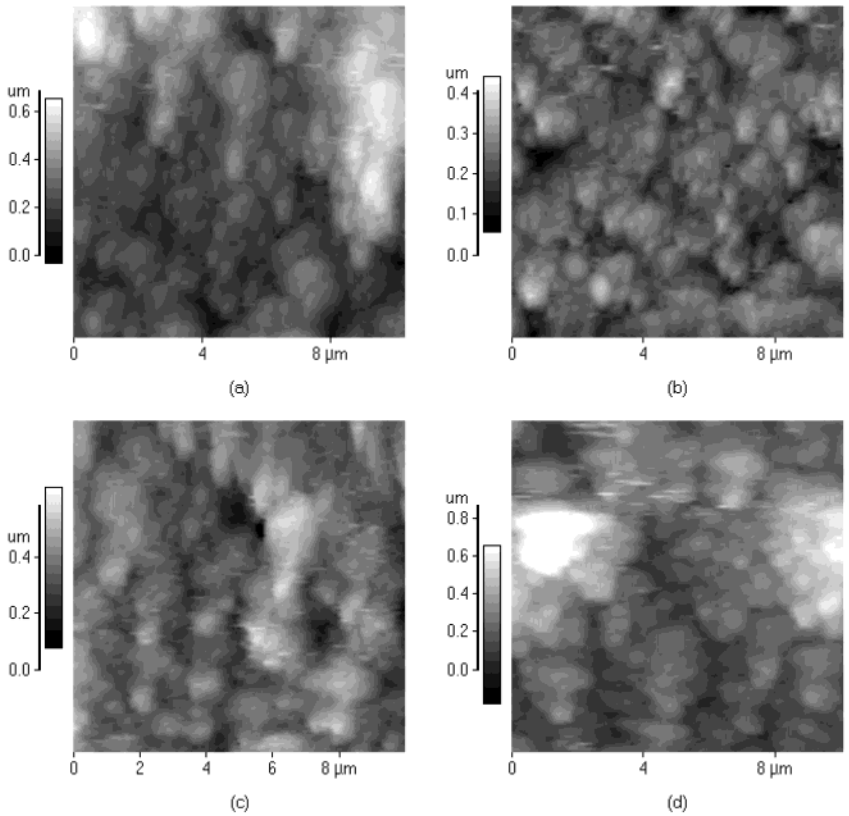

Figure 5. AFM images of 120 bilayers of PSS/TiO_2 film before (a) and after sintering (b) and of 120 bilayers of PDAC/TiO_2 film before (c) and after sintering (d). The short white lines in the images come from the scan defects since the multilayered nanocomposite films have very uneven surfaces.

after sintering are presented in parts a and b of Figure 5, and those for 120 bilayers of (PDAC/TiO_2) multilayer film are presented in parts c and d of Figure 5, respectively. Very similar AFM images have been observed for multilayered PAH/TiO_2 and PAA/TiO_2 films before and after sintering. Comparing these images to the AFM images of 1-bilayer films in Figure 4, we can see from the height scale that the surface roughness increases from nanometer range to micron range due to the formation of thicker films. Larger polyelectrolyte/TiO_2 aggregates are present in the multilayer films, which indicates that the polyelectrolytes indeed play a role to bind TiO_2 nanoparticles. Compared to the images before and after sintering, the particle size and morphology did not show obvious change except that the particles become a little bit clearer after sintering due to the thermal degradation of the "soft" polyelectrolytes.

3.2. Photovoltaic Measurements. Since the thicknesses of these polyion/TiO_2 films are well controlled, these nanocomposite ELBL films are ideal structures to investigate the relationship between the performance of DSSCs and the thickness of TiO_2 films. The DSSCs have been made from multilayered polyion/TiO_2 films which are sintered at 550 °C for 30 min. After sintering, the thickness of the films does not show a noticeable change. The $I-V$ curves of the DSSCs made from PSS/TiO_2 precursor films are presented in Figure 6. From the figure, we can see that the overall energy conversion efficiency increases from 1.40% to 4.32% with the thickness increase of TiO_2 films. The increase of cell efficiency is mainly due to the increase of the short-circuit photocurrent (Isc) which indicated that more N3 dye has been adsorbed on the thicker polyion/TiO_2 film. However, the dependence of the cell efficiency on the thickness of polyion/TiO_2 film does not follow a linear relationship. From 120 bilayers to 160 bilayers of

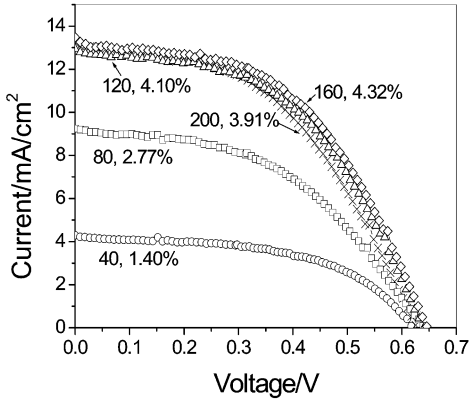

Figure 6. $I-V$ curves of solar cells made from PSS/TiO_2 films with different thicknesses.

PSS/TiO_2 as the precursor film, the cell efficiency increases only from 4.10 to 4.32%. Furthermore, for a 200-bilayer film, the cell efficiency was observed to even decrease to 3.91%.

The decrease of cell efficiency is unexpected since the amount of N3 dye continues to build up with the increase of film thickness, as observed in Figure 7, which shows the difference absorption spectra before and after N3 adsorption during sequential buildup of the PSS/TiO_2 film. The linear increase of absorbance at 530 nm, as shown in the inset, indicates that the amount of N3 increases linearly with the film thickness. The nonlinear dependence of the cell efficiency on the film thickness is not in agreement with the linear increase in dye adsorption. This trend also appears when other polyelectrolytes, PAA, PAH, and PDAC, are used. Table 1 lists the $I-V$ characteristics of the cells made from different thicknesses of PAA/TiO_2, PAH/TiO_2, and PDAC/TiO_2 films. Generally, for all

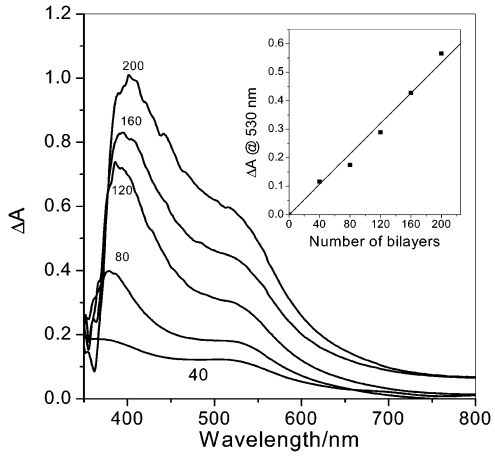

Figure 7. Difference absorption spectra (before and after N3 adsorption) of N3-sensitized PSS/TiO_2 films. The inset shows the absorbance change at 530 nm with the number of bilayers.

Table 1. *I*−*V* Performances of Photovoltaic Devices Made from PAA/TiO_2, PAH/TiO_2, and PDAC/TiO_2 Nanocomposite Films

no. of bilayers	Imax (mA/cm^2)	Vmax (V)	Jsc (mA/cm^2)	Voc (V)	FF	η (%)
			PAA			
40	1.41	0.55	1.97	0.69	0.57	0.78
80	4.28	0.52	5.00	0.70	0.64	2.23
120	6.52	0.53	7.65	0.71	0.64	3.46
160	7.44	0.51	8.60	0.68	0.65	3.79
200	9.40	0.50	11.01	0.68	0.63	4.70
240	8.04	0.50	9.25	0.68	0.64	4.02
			PAH			
40	4.84	0.52	5.78	0.71	0.61	2.52
60	7.64	0.50	9.03	0.69	0.61	3.82
80	9.55	0.49	11.49	0.68	0.60	4.68
100	10.57	0.47	12.77	0.69	0.56	4.97
120	12.02	0.48	14.45	0.7	0.57	5.77
180	12.55	0.46	14.93	0.68	0.57	5.77
300	11.82	0.48	14.63	0.68	0.57	5.67
			PDAC			
40	6.20	0.46	9.28	0.66	0.46	2.82
80	12.84	0.48	15.67	0.69	0.57	6.20
120	14.15	0.46	16.49	0.69	0.57	6.51
160	14.84	0.46	17.39	0.68	0.58	6.84
200	15.56	0.46	20.30	0.68	0.52	7.22

polyelectrolytes used, a nonlinear increase of cell efficiency with film thickness is observed with an optimized film thickness for maximum conversion efficiency. Also, the cell efficiency is larger when using polycationic PAH and PDAC as binders compared to using polyanionic PAA and PSS. Typically, a 7.2% efficiency was obtained with a 200-bilayer PDAC/TiO_2 film while a 200-bilayer PAA/TiO_2 film gave an efficiency of 4.7%. The adsorbed dye amount for four different polyelectrolyte/TiO_2 films was measured to be 16 ± 2 mg of N3 per gram of polyelectrolyte/TiO2 complex; that is, the dye loading densities in these films are the same. On the basis of these observations, we conclude that factors other than the amount of dye adsorption are playing a role in the cell efficiency in these types of polyion/TiO_2 films.

Another key component of these nanocomposite films is the polyelectrolytes. Since these polyelectrolytes are insulators, if the high-temperature sintering process does not completely burn away all of these materials, the residuals left inside the TiO_2 film can increase the internal resistance of the solar cell which in turn will reduce the photocurrent output. On the basis of this consideration, the thermal stabilities of the polyelectrolytes were tested by TGA and are shown in Figure 8. Under the sintering temperature of 550 °C, the weight losses of PSS, PAA, PDAC, and PAH are ca. 18%, 50%, 87%, and 94%, respectively. In other words, the residuals of the polyanions left in the final TiO_2 electrodes are significantly more than those of the polycations after sintering. Due to the insulating property of the residuals inside the final TiO_2 electrodes, the more residual the film has, the poorer the performance of the cell. The TGA data support this since significantly high cell efficiency is obtained with the polycation-based TiO_2 films. Therefore, it can be concluded that the thermal stability of the polyelectrolyte plays a major role in the cell performance for polyion/TiO_2 nanocomposite films.

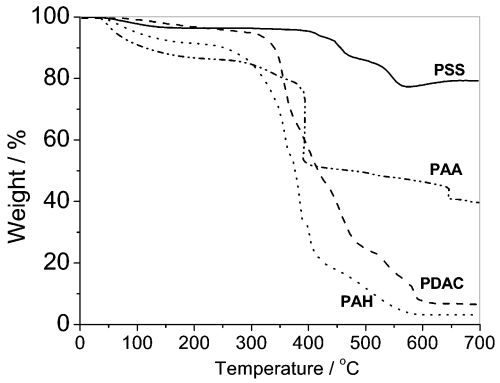

Figure 8. TGA of PSS, PAA, PDAC, and PAH under an air atmosphere. The heating rate is 10 °C/min.

To improve the cell performance, a way to enhance the oxidization of the polyelectrolytes in the nanocomposite films has been carried out by sintering these films at 550 °C under an oxygen atmosphere. In comparison to samples sintered under ambient atmosphere, the cell performance did not show substantial change. We think the reason may be that the oxidized residuals of polyelectrolytes have been trapped inside the cross-linked TiO_2 film and cannot easily escape. Further efforts to improve the performance of the cells made by the ELBL TiO_2/polyion films are ongoing in our laboratory.

4. Conclusion

In this work, it has been demonstrated that ELBL assembly may be used as an alternative approach to fabricate nanocrystalline TiO_2 electrodes for DSSC applications. The solar cell efficiency obtained with this method is comparable to that with conventional coating methods. The advantages of the ELBL technique, such as versatility, thickness, composition, and porosity control, are expected to provide many new opportunities for the design and fabrication of efficient dye-sensitized solar cells.

Acknowledgment. This work was supported by the U.S. Army Natick Soldier Center, SBCCOM.

LA020639B